J Mater Sci
DOI 10.1007/s10853-013-7540-1

# Glassy magnetic behavior in the metamagnetic $DyAlO_3$ doped with Cr

**R. Escudero · B. L. Ruiz-Herrera · M. P. Jimenez · F. Morales**

Received: 1 April 2013 / Accepted: 14 June 2013


**Abstract** Magnetic properties of $DyAl_{0.926}Cr_{0.074}O_3$ and $DyAlO_3$ were studied. We found that both the compounds are antiferromagnetic with a low Néel transition temperature. At higher temperatures the magnetic characteristics show a Curie–Weiss dependence. Néel temperature disappears when a field of about 2 T is applied, the system changes from an antiferromagnetic to a weak ferromagnetic behavior due to a metamagnetic transition. Furthermore, AC magnetic measurements in the Cr-doped compound, at different frequencies, show a spin glass-like behavior. These transitions were studied and corroborated by specific heat measurements. We found the presence of metamagnetism and spin glass in the compound doped with chromium, determining that the small addition of chromium atoms modifies the magnetic properties of the compound $DyAlO_3$, resulting in new features such as the spin glass-like behavior.

## Introduction

The large family of compounds known as perovskites has a simple crystal structure, related to the mineral $CaTiO_3$. This family forms an enormous variety of compounds with a very rich variant in its chemical and physical properties. The base compound, $ABX_3$ type, presents a cubic crystal structure in its ideal form. This can be described as corner sharing $BX_6$ octahedral, where A cation, that is in the middle of the structure, has 12-fold coordination site [1, 2].

R. Escudero · B. L. Ruiz-Herrera · M. P. Jimenez · F. Morales (✉)
Instituto de Investigaciones en Materiales, Universidad Nacional Autónoma de México, 04510 Mexico, DF, Mexico
e-mail: fmleal@unam.mx

Perovskites show many structural modifications that according to the used atoms give place to a great variety of magnetic and electronic characteristics. An example of a compound whose structure present a distortion of the ideal perovskite form is the orthorhombic $DyAlO_3$ [3, 4], which magnetic behavior is widely known [5–10], and interpreted from the viewpoint of the Anderson model of magnetic exchange in insulators, with a mechanism of indirect exchange between the nearest Dy ions [11].

According to neutron diffraction study of the compound [10], the dysprosium atoms form a magnetic structure of type $G_xA_y$, in Bertaut's notation, which corresponds to the space group *Pbnm*. Magnetic order generated by dysprosium resembles two antiferromagnetic networks embedded, one of them canted relative to one another. $DyAlO_3$ has this antiferromagnetic behavior below $T_N \sim 3.5$ K. Moreover, $DyAlO_3$ exhibits a metamagnetic transition that is related to an abrupt change of one or more magnetic sublattices under an applied field [5, 7, 8].

The subclass of magnetic materials known as the spin glass materials consist in a mixed-interacting magnetic system formed by magnetic moments randomly located in a lattice, leading to multidegenerate ground states but also a cooperative freezing transition at a well-defined temperature, the freezing temperature $T_f$ [12–14].

At high temperature all magnetic moments in a spin glass are independent. As the temperature decreases some spins build up into locally correlated units, spins that are not included in this formed clusters take part interacting between them. Finally, at $T_f$ the system achieve one of its many ground states and freezes, process that is understood as a cooperative effect. Consequently, below $T_f$ a spin glass posses metastability reflecting in a divergence between the field-cooled and zero field-cooled magnetic susceptibility below $T_f$, among other features.

Published online: 25 June 2013

Perovskites of the type $TRMO_3$ (TR = rare earth, M = transition metal) with partial substitution of the transition metal or the rare earth show spin glass behavior [15–17]. $DyAlO_3$ is an antiferromagnetic material and its magnetic behavior with partial substitutions has not been determined yet.

In this paper, we report magnetic measurements on the orthorhombic perovskites: $DyAl_{0.926}Cr_{0.074}O_3$ and $DyAlO_3$. The small amount of Cr was eventually used to observe the behavior of the compound, and also in other lanthanide perovskites as magnetic pigments; however, we must stress that the spin glass behavior was a serendipitous discover, and was only observed in this compound, more different compositions will be studied in the future. Magnetic properties were carried out by DC and AC molar susceptibility measurements. The DC susceptibility was measured at different magnetic fields and temperatures, meanwhile the AC susceptibility was performed as function of temperature and frequency. In addition, specific heat measurements as function of temperature and magnetic field were performed. The main results of this report are that in the doped compound the metamagnetism persists and a spin glass behavior is developed below 3.2 K. We analyze the spin glass-like behavior using the conventional critical slowing-down spin dynamics.

## Experimental details

The materials used for the synthesis were: $Dy_2O_3$, $Al(NO_3)_3{\cdot}9H_2O$, and $Cr_2O_3$ provided by J. T. Baker. Compounds were prepared by mixing the starting materials in the relations to the chemical formula: $DyAl_{0.93}Cr_{0.07}O_3$ and $DyAlO_3$. All powders were mixed in an agate mortar. Platinum crucibles were used. Residual compounds as water and nitrogen oxides were eliminated by the thermal treatment. Samples were annealed in a furnace at 900 °C in a period of 24 h, after this first treatment the resulting powders were fired at temperatures about 1000 °C in a period of 96 h. Samples were characterized by X-ray powder diffraction (XRD) with a Siemens D5000 diffractometer, using Co $K_{\alpha 1}$ wavelength and a secondary graphite monochromator. Measurements were carried out on the $2\theta$ range from 5° to 110°. Rietveld analysis [18] was performed, using the *Fullprof* software, in order to distinguish more clearly the influence of chromium atoms and characterization of all crystal cell parameters.

Magnetic measurements were performed using a Magnetic Properties Measurements System (MPMS) Quantum Design magnetometer. The range of measured temperature was from 2 to 300 K and the applied magnetic field was about ±5 T. Measurements were performed in zero field cooling (ZFC) and field cooling (FC) modes. Isothermal magnetic measurements were performed between ±5 T, for sample doped with Cr at 2 and 3.2 K and for $DyAlO_3$ at 2 and 5 K. AC magnetic measurements were performed, in both compounds, with an applied magnetic field of 1 Oe and frequencies from 50 to 1000 Hz. Furthermore, specific heat $C_P$ measurements were performed in a PPMS of Quantum Design at zero magnetic field and high magnetic fields up to 9 T. In these measurements, the specific heat addenda, sample support and grease, were extracted to obtain the absolute $C_P$ of the sample.

## Results and discussion

### Structural characterization

The examination of X-ray diffractograms shows that the perovskite-based structures $DyAl_{0.93}Cr_{0.07}O_3$ and $DyAlO_3$ have orthorhombic symmetry with *Pbnm* space group. Figure 1 shows the results of the Rietveld refinement, and Table 1 contains the crystallographic data of the samples. The occupation factor reveals that the chromium resides in the same position of aluminum atoms in the unit cell, besides, give us information about the quantity of Al ions that are being substituted by Cr. Accordingly, the stoichiometry changes gave the resulting formula $DyAl_{0.926}Cr_{0.074}O_3$. This will be used as the real stoichiometry in all the text. The polycrystalline phases were identified by comparison with X-ray patterns in the Inorganic Crystal Structure Database (ICSD) 2012. All peaks correspond to the $DyAlO_3$ phase [4], except the peaks related to $Dy_2O_3$ found in low proportion in the compound; however, according to our results this impurity is not affecting the observed magnetic characteristics. Rietveld refinement was made using crystallographic data of the isostructural compound $GdAlO_3$ (ICSD 59848) and $Dy_2O_3$ (ICSD 82421). In the distorted perovskites, $Al^{3+}$ and $Cr^{3+}$ ions remain essentially in octahedral sites; thus, when $Al^{3+}$ is substituted by $Cr^{3+}$, which is about 12.3 % bigger than the size of $Al^{3+}$, the Al–O distance decreases. Despite the inclusion of chromium, the volume of unit cell does not present a considerable change, only about 0.4 %.

### Magnetic measurements

In Fig. 2, the main panel displays the magnetic susceptibility, $\chi(T)$, for the compound $DyAl_{0.926}Cr_{0.074}O_3$, from 50 to 2 K at six different magnetic fields. It could be thought that the peak at about 3.2 K is only the signature of an antiferromagnetic transition, $T_N$, due that the undoped compound has a similar transition at 3.55 K corresponding to Néel temperature [8, 10]. However, a careful observation shows that the peak is quite broad, and also the size of the peak is very dependent of the intensity of the applied

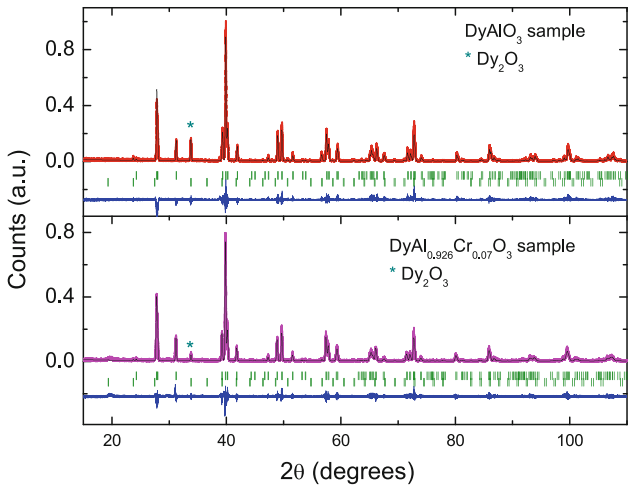


**Fig. 1** (Color online) Rietveld refinement of the $DyAlO_3$ and $DyAl_{0.926}Cr_{0.074}O_3$ samples. *Red* and *purple lines* are the experimental data, the *superposed black line* is the calculated pattern. At the bottom of each diagram, the difference between experimental and calculated data is shown in *blue line*. *Vertical green marks* are displayed in two rows, *upper ones* correspond to the Bragg positions for $DyAlO_3$ and *lower ones* to $Dy_2O_3$ patterns

magnetic field: it is smoothed with increasing field and finally at 2 T it disappears. Thus, accordingly to this, the peak may be related to an antiferromagnetic transition with another physical process associated.

The upper inset in Fig. 2 shows measurements in ZFC and FC modes at low temperature. The different behavior of the ZFC and FC curves, besides the width of the peak, suggests us a spin glass behavior. Careful examination of $\chi(T)$ measurements at 5 T shows a negative curvature at low temperature, clearly seen in the main panel and in the lower inset of Fig. 2. This change must be compared with the curves measured at 0.001, 0.01, 0.1, and 0.5 T. The change of curvature is also an indication of a metamagnetic transition induced by the magnetic field; thus, a change from canted antiferromagnetism to a weak ferromagnetism.

The inverse of the susceptibility $\chi(T)^{-1}$ of $DyAl_{0.926}Cr_{0.074}O_3$ provides more information about the magnetic behavior. The experimental data above 100 K were fitted (continuous line) with the Curie–Weiss law, as illustrated in Fig. 3. From the fitting, we obtain the Curie constant, $C$, and the Curie–Weiss temperature, $\theta_{CW}$. Measurements of the specimen in 0.001 T give $C = 10.6$ cm$^3$ K mol$^{-1}$, and $\theta_{CW} = -7$ K; whereas, the measurement performed at 5 T gives $C = 12.62$ cm$^3$ K mol$^{-1}$, and $\theta_{CW} = -3.4$ K. Those changes in the constants can be correlated to the shift of the magnetic behavior in a very clear manner. Magnetic effective moments, $\mu_{eff}$, Curie constants, and Curie–Weiss temperatures are slightly dependent on the applied magnetic field, showing only very small changes: for low field, 0.001 T, $\mu_{eff} = 9.6\ \mu_B$, whereas for

**Table 1** Crystallographic data for $DyAl_{0.926}Cr_{0.074}O_3$ and $DyAlO_3$ obtained by Rietveld refinement. Symmetry is described by the orthorhombic space group *Pbnm*; standard deviations are written between parentheses

| Rp (%) | Rwp (%) | Re (%) | $\chi^2$ | |
|---|---|---|---|---|
| 20.7 | 29.8 | 24.81 | 1.44 | |
| Parameters (Å): | $a$ = 5.33423(3) | $b$ = 7.40830(4) | $c$ = 5.21155(3) | |
| Volume (Å$^3$): | 205.948(0.002) | | | |
| $DyAl_{0.926}Cr_{0.074}O_3$ | | | | |
| Site | $x$ | $y$ | $z$ | Occupation |
| Al | 0 | 0 | 0 | 0.463(3) |
| Dy | 0.44982(11) | 0.25000(0) | −0.00999(21) | 0.500(0) |
| O1 | 0.02531(121) | 0.25000(0) | 0.07013(136) | 0.500(0) |
| O2 | 0.29257(108) | −0.04074(76) | 0.21421(115) | 1.000(0) |
| Cr | 0 | 0 | 0 | 0.037(3) |
| | $DyAl_{0.926}Cr_{0.074}O_3$ | $Dy_2O_3$ | | |
| Phase fraction (%) | 98.10(0.29) | 1.90(0.04) | | |
| Rp (%) | Rwp (%) | Re (%) | $\chi^2$ | |
| 22.0 | 29.8 | 23.28 | 1.63 | |
| Parameters (Å) | $a$ = 5.31986(3) | $b$ = 7.40187(5) | $c$ = 5.21007(3) | |
| Volume (Å$^3$) | 205.157(0.002) | | | |
| $DyAlO_3$ | | | | |
| Site | $x$ | $y$ | $z$ | Occupation |
| Al | 0 | 0 | 0 | 0.500(0) |
| Dy | 0.45209(11) | 0.25000(0) | −0.00953(20) | 0.500(0) |
| O1 | 0.00769(112) | 0.25000(0) | 0.06031(134) | 0.500(0) |
| O2 | 0.28016(115) | −0.03580(74) | 0.21425(106) | 1.000(0) |
| | $DyAlO_3$ | $Dy_2O_3$ | | |
| Phase fraction (%) | 93.27(0.26) | 6.73(0.06) | | |

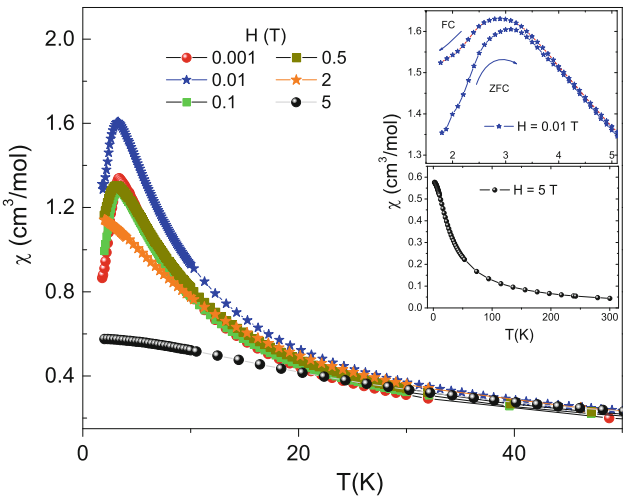


**Fig. 2** (Color online) $\chi(T)$ in ZFC mode for the compound $DyAl_{0.926}Cr_{0.074}O_3$ determined at several magnetic fields from 0.001 to 5 T. The *main panel* shows $\chi(T)$ from 2 to 50 K. The *peak* observed at *low field* indicates the antiferromagnetic transition at about 3.2 K. The *upper inset* displays the irreversible behavior of the curve with measurements performed in FC and ZFC modes at 0.01 T. *Lower inset* shows the behavior at $H = 5$ T in ZFC mode from 2 to 300 K

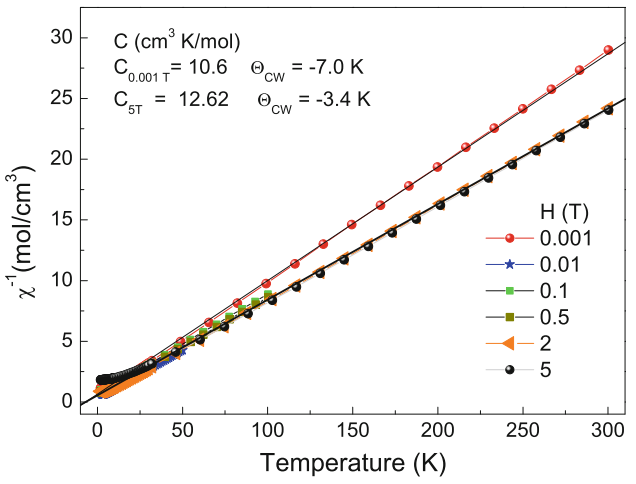


**Fig. 3** (Color online) Inverse of the magnetic susceptibility, $\chi(T)^{-1}$ measured at different magnetic fields for $DyAl_{0.926}Cr_{0.074}O_3$. *Lines* on the experimental data are the fitting to the Curie–Weiss law at two fields, 0.0001 and 5 T. *C*'s are the Curie constants, and Curie–Weiss temperatures are the resulting values of the fitting

5 T $\mu_{eff} = 10.03\ \mu_B$. These values are similar to the theoretical value of $Dy^{3+}$ of 10.65 $\mu_B$. Experimental values of $\mu_{eff}$ of $DyAlO_3$ reported are 9.2 $\mu_B$ [6] and 0.38 $\mu_B$ in nanocrystals [5].

Figure 4 shows the magnetization as a function of magnetic applied field $M(H)$ at 2 K, below Néel temperature. When the field is increased and decreased for the doped and pure compounds, shown in the top and bottom panels, respectively, a slope change is observed about ±10 kOe, this change corresponds to the metamagnetic transition. This transition agrees well to previously reported one for $DyAlO_3$ [5]. We must stress the persistence of the metamagnetism in the Cr-doped compound, although it is quite reduced. The reduced metamagnetism in the doped compound compared to the undoped one may be explained by the distortions created by the Cr magnetic moment. The small amount of Cr introduces small distortions in the magnetic structure in the three magnetic subcells of the compound, but without completely destroying the metamagnetic behavior. The Cr introduces disorder that modify the magnetic interactions between Dy atoms. Moreover, it is shown that saturation magnetization of compound doped with Cr is higher than nondoped one.

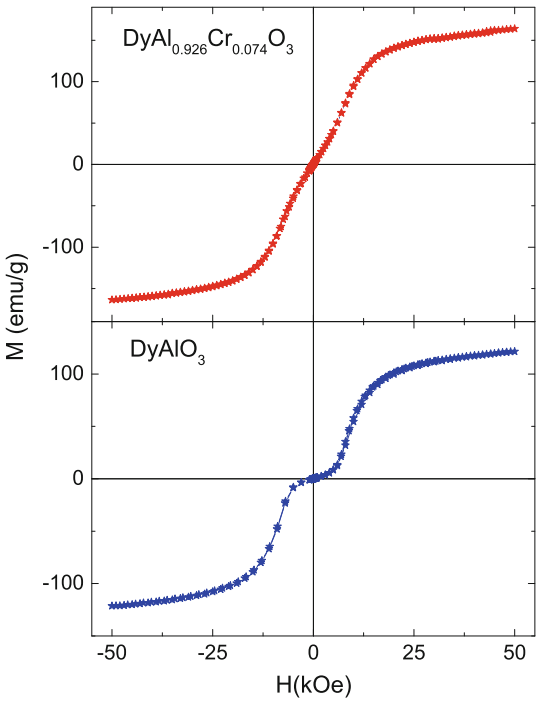


**Fig. 4** (Color online) The *top panel* presents the metamagnetic change of the doped Cr compound in $M(H)$, whereas the *bottom panel* displays the well-known metamagnetic transition of $DyAlO_3$. Data of two panels were taken at 2 K below Néel temperature. It is interesting to compare both figures; in the Cr-doped sample, the metamagnetic behavior is clearly seen but quite reduced as compared with the pure compound

## Specific heat and AC susceptibility

Specific heat measurements provide information about magnetic transitions. The specific heat of $DyAlO_3$ has a transition lambda type at about 3.5 K [9, 19], in agreement to the magnetic measurements. The transition observed in $DyAl_{0.926}Cr_{0.074}O_3$ (Fig. 5) is not of the lambda type, suggesting that Cr produces some effect on the magnetic order. Figure 5 presents specific heat measurements at two magnetic fields: 0 and 5 T. The main panel displays these

measurements from 2 to 50 K. The red curve (triangles) shows the measurements at zero magnetic field, whereas the black dots are the measurements with field at 5 T. Two important changes must be noted: at zero field and low temperature a peak is clearly seen and is associated with the antiferromagnetic transition, this peak was also seen in the $\chi(T)$ measurements. However, with 5 T the peak at low temperature disappears, and a small bump is present at about 38–40 K.

Assuming that $DyAl_{0.926}Cr_{0.074}O_3$ is an electric insulator the specific heat data were fitted between 3.1 and 10 K with the following equation [20]:

$$C_P = \alpha T^{-2} + \beta_3 T^3 + \beta_5 T^5 + \beta_7 T^7,$$

the first term represents the contribution to $C_P$ because of the short-range-order effect of the spin alignment when $T$ approach to $T_N$ from high temperature [21]. The second term is the harmonic contribution of the lattice vibrations, whereas the last two terms are due to quasi-harmonic contributions to the specific heat [22]. Those terms give $\beta$ values very small but important in the case of anharmonicity produced by impurities or disorder as we considered for the case produced by the chromium atoms. The upper inset in Fig. 5 displays the curve portion of $C_P - T$ data and the obtained fit, continuous line. From the fitting, we obtain: $\alpha = (30.88 \pm 0.374)$ J K/mol; $\beta_3 = (0.00181 \pm 8.8 \times 10^{-5})$ J/mol K$^4$; $\beta_5 = (-7.86 \times 10^{-6} \pm 8.6 \times 10^{-7})$ J/mol K$^6$; $\beta_7 = (1.23 \times 10^{-8} \pm 1.86 \times 10^{-9})$ J/mol K$^8$. Using the Debye approximation; $\beta_3 = 1973.7 s \theta_D^{-3}$, where $s$ is the number of atoms per formula unit, we obtain $\theta_D = 175$ K, in agreement to $\theta_D$ values reported for $DyAlO_3$ [23, 24]. The lower inset of Fig. 5 displays the magnetic effect on the anomalous peak associated to Néel temperature. Note the variation of the size of the peak as the field is increased, this peak is quite width and behaves differently to normal antiferromagnetic peak. In fact this anomalous shape take us to perform AC magnetization measurements as a function of frequency, study that is showed in the last part of this section.

Figure 6 shows the influence of the magnetic field in specific heat measurements at temperatures between 50 and 25 K; in this figure, we plotted $C_P/T$ versus $T$. In this temperature range, two bumps arise with a field of 2 T, at temperature about 37.3 and 43.4 K, increasing in size as the magnetic field was increased. It is necessary to remark that in the curve measured at zero field there is no feature at all. We must also mention that a Schottky anomaly reported in $Dy_2O_3$ at 45 K could be related to this feature [25]; however, it is also clear that if the Schottky anomaly has some influence this necessary will be present without magnetic field. Because of the magnetic measurements do not show any one feature, at around the temperatures where the bumps are observed in $C_P(T)$, we think that these bumps could be related to a structural modification produced by the magnetic field, as was observed on single crystals of $DyCrO_3$ [26].

Figure 7a and b displays the real part $\chi'$ and imaginary part $\chi''$ of the AC susceptibility as a function of temperature and frequency, $f$, of the doped compound. The measurements were performed at seven different frequencies. The maximum of $\chi'(T)$ displaces to higher temperatures as the frequency increases. This behavior has been associated

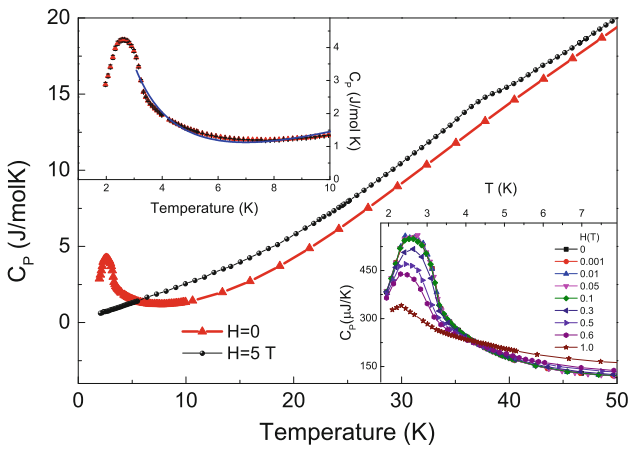


**Fig. 5** (Color online) The *main panel* displays the specific heat of $DyAl_{0.926}Cr_{0.074}O_3$ from 2 to 50 K at two magnetic fields: 0 and 5 T. Note the suppression of the Néel peak at low temperature, but also a bump at a temperature about 38 K at $H$ = 5 T. *Top inset* shows a fitting (*continuous line*) of the data at low temperatures. The *bottom inset* displays a close view of the influence of the magnetic field and the suppression of the peak at 2.3 K

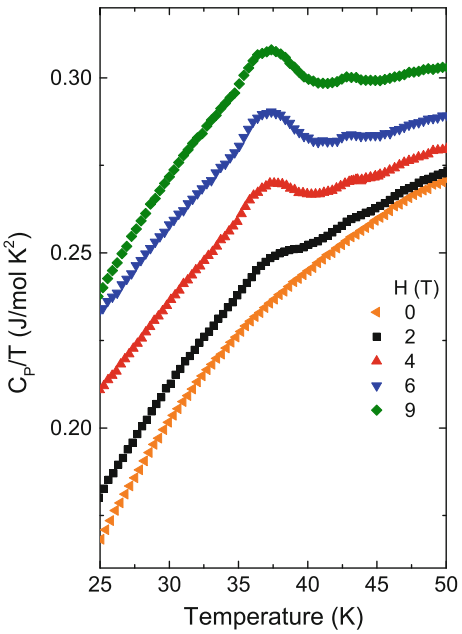


**Fig. 6** (Color online) Plot of $C_P/T - T$ from 50 to 25 K of $DyAl_{0.926}Cr_{0.074}O_3$, measured at different magnetic fields, from 0 up to 9 T. It is clearly seen a bump arising at a temperature about 37.3 K and a smoother one around 43 K

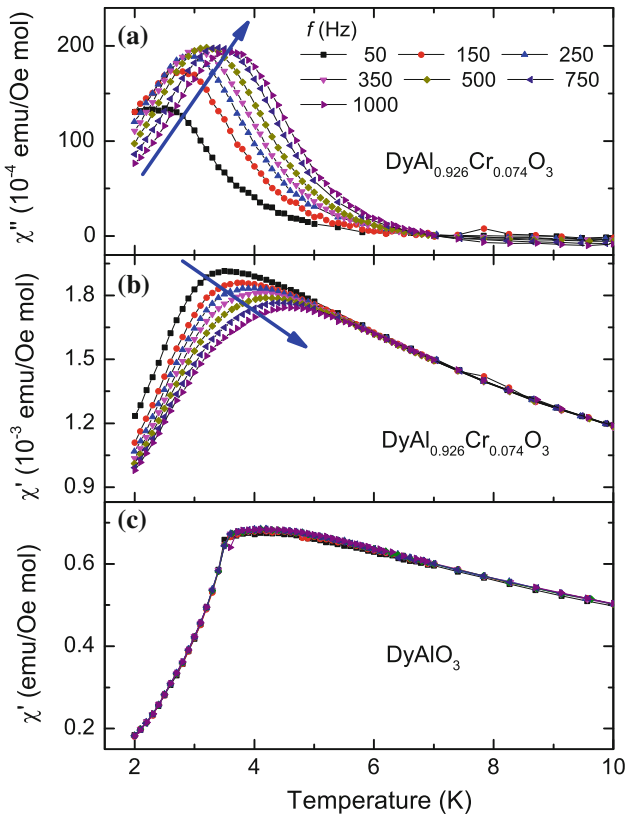


**Fig. 7** (Color online) Imaginary part (**a**) and the real part (**b**) of the AC susceptibility of $DyAl_{0.926}Cr_{0.074}O_3$, at different frequencies showing spin glass characteristics. **c** shows the real part of the AC susceptibility $\chi'(T)$ of $DyAlO_3$

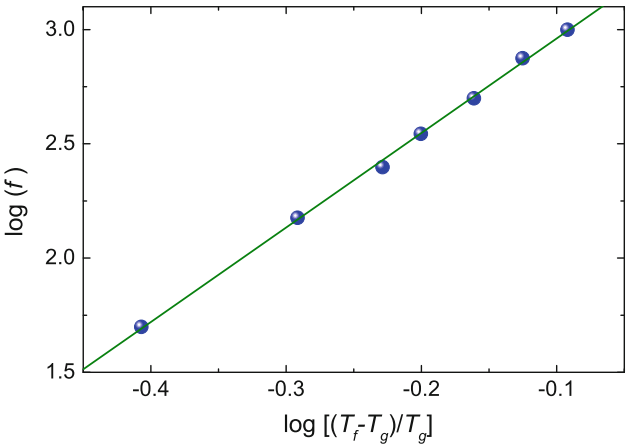


**Fig. 8** (Color online) Dynamic scaling of the critical slowing down of the compound $DyAl_{0.926}Cr_{0.074}O_3$ extracted from $\chi'(T)$ data at various frequencies $f$

to spin glass systems. It is noteworthy that above 6 K, $\chi'(T)$ becomes frequency independent. Figure 7c displays $\chi'(T)$ of $DyAlO_3$, its behavior belongs to an antiferromagnetic material. There is not a frequency effect on the maxima of the AC susceptibility, demonstrating that the insertion of Cr in the lattice provokes spin glass behavior. It is noteworthy to mention that there are few previous studies where spin glass, antiferromagnetism, and metamagnetism are present in the same specimen.

AC susceptibility measurements as a function of frequency permit to obtain information about the dynamic behavior of spin glasses using the standard critical slowing-down formula [13]:

$$\frac{\tau}{\tau_0} = \left(\frac{T_f - T_g}{T_g}\right)^{-zv},$$

where $\tau = (2\pi f)^{-1}$ is the relaxation time, $zv$ is a critical exponent, and $\tau_0$ is a microscopic relaxation time corresponding to the shorter time available to the fluctuations. $T_f$ is the freezing temperature, defined as the temperature at the maximum of $\chi'(T)$, meanwhile $T_g$ is the critical temperature for spin glass ordering equivalent to $T_f(\omega)$ as $\omega \to 0$ [27, 28]. The main panel of Fig. 8 displays $\log(f)$ versus $\log[(T_f - T_g)/T_g]$ for the different frequencies used in the AC susceptibility measurements. The straight line is the best fit to the data obtained with: $T_g \simeq 2.5$ K, $zv \simeq 4.1$, and $\tau_0 \simeq 6.7 \times 10^{-5}$ s. The value of $zv$ for several spin glasses is between the values 4 and 12 [29]. However, the values expected for $\tau_0$ in conventional spin glass are of the order of $10^{-13}$ s, shorter than the value obtained for $DyAl_{0.926}Cr_{0.074}O_3$. $\tau_0$ values of the order of $10^{-10}$ s have been reported in systems where formation of glazing clusters with ferromagnetic order [16, 30]. Values of $\tau_0 \sim 10^{-5}$ and $zv \approx 1$ have been reported in compounds where two dynamical freezing processes are in the same system [31].

DC and AC magnetization measurements on $DyAl_{0.926}Cr_{0.074}O_3$ at low temperature and low magnetic field suggest that antiferromagnetism and spin glass coexists below $T_g$. As mentioned before the antiferromagnetic state was produced by the Dy sub-cells and the spin glass is produced by the Al network with Cr impurities. One last point worth to mention is the fact that the DC magnetic measurements at low field, in the Cr-doped compound, show $T_N = 3.1$ K, whereas the analysis of the relation of frequency and the freezing temperature gives $T_g = 2.5$ K that coincides with the maximum of $C_P(T)$ at low field and low temperature.

## Conclusions

Two Dy orthoaluminate perovskites with space group *Pbnm*, formulae $DyAlO_3$ and $DyAl_{0.926}Cr_{0.074}O_3$, were studied and compared. The Cr-doped compound maintains the metamagnetic transition observed in $DyAlO_3$, but quite reduced and changing from an antiferromagnetic behavior to a weak ferromagnetism. The AC susceptibility measurements indicate an unusual spin glass-like behavior as

the dynamic analysis shows; a long relaxation time that indicates the presence of two dynamical freezing processes. This different behavior respect to other spin glasses may be because the complicated magnetic structure of the compound, as already studied by other researchers. Interesting magnetic features were observed in the specific heat measurements at about 35–45 K, with increasing magnetic field. These magnetic anomalies observed in our specific heat measurements are indicative of the complicated magnetic structure of the compound. All these observations situate the $DyAl_{0.926}Cr_{0.074}O_3$ as an uncommon glassy compound that requires further investigations.

**Acknowledgements** Partial support for this work is gratefully acknowledged to CONACyT Project 129293 (Ciencia Básica), DGAPA-UNAM Project No. IN100711, Project BISNANO 2011, and Project PICCO 11-7 by The Institute of Sciences of Distrito Federal, Ciudad de México. We thank Mr. R. Reyes, for help in technical assistance, and Dr. C. Piña for the initial prepared samples.

## References

1. Johnsson M, Lemmens P (2007) In: Kronmüller H, Parkin S (eds) Handbook of magnetism and advanced magnetic materials. Wiley, Chichester, p 2098
2. Bhalla AS, Guo R, Roy R (2000) Mater Res Innovat 4:3
3. Vasylechko L, Senyshyn A, Bismayer U (2009) In: Handbook on the physics and chemistry of rare earths, vol 39. North-Holland Publishing, Amsterdam, p 113
4. Dalziel JAW, Welch AJE (1960) Acta Cryst 13:965
5. Petrov D, Angelov B, Lovchinov V (2011) J Sol–Gel Sci Technol 58:636
6. Holmes LM, Van Uitert LG, Hecker RR, Hull GW (1972) Phys Rev B 5:138
7. Holmes LM, Van Uitert LG (1972) Phys Rev B 5:147
8. Schuchert H, Hüfner S, Faulhaber R (1969) Z Phys 222:105
9. Cashion JD, Cooke AH, Thorp TL, Wells MR (1968) J Phys C 1:539
10. Bidaux A, Meriel P (1968) J Phys 29:220
11. Petrov D, Angelov B (2011) Acta Phys Pol A 122:737
12. Mydosh JA (1993) Spin glasses: an experimental introduction. Taylor and Francis, London
13. Binder K, Young AP (1986) Rev Mod Phys 58:801
14. Blundell S (2011) Magnetism in condensed matter. Oxford University Press, New York
15. Pérez J, García J, Blasco J, Stankiewicz J (1998) Phys Rev Lett 80:2401
16. Nam DH, Mathieu R, Nordblad P, Khiem NV, Phuc NX (2000) Phys Rev B 62:8989
17. Motohashi T, Caignaert V, Pralong V, Hervieu M, Maignan A, Raveau B (2005) Phys Rev B 71:214424
18. Young RA (1993) The Rietveld method. Oxford University Press Inc., New York
19. Tanaeva IA, Ikeda H, van Bokhoven LJA, Matsubara Y, de Waele ATAM (2003) Cryogenics 43:441
20. Tari A (2003) The specific heat of mater at low temperatures. Imperial College Press, London
21. Miyazaki Y, Wang Q, Yu Q-S, et al. (2005) Thermochim Acta 431:133
22. Dugdale JS, MacDonald DKC (1954) Phys Rev 96:57
23. Cashion JD, Wells MR (1998) J Magn Magn Mater 177–181:781
24. Kuz'min MD, Tishin AM (1993) J Appl Phys 73:4083
25. Gruber JB, Chirico RD, Westrum Jr EF (1982) J Chem Phys 76:4600
26. Krynetskiĭ IB, Matveev VM (1997) Phys Solid State 39:584
27. Gunnarsson K, Svedlindh P, Nordblad P, Lundgren L, Aruga H, Ito A (1988) Phys Rev Lett 61:754
28. Malinowski A, Bezusyy VL, Minikayev R, Dziawa P, Syryanyy Y, Sawicki M (2011) Phys Rev B 84:024409
29. Imamura N, Karppinen M, Motohashi T, Yamauchi H (2008) Phys Rev B 77:024422
30. Tang Y-K, Sun Y, Cheng Z-H (2006) Phys Rev B 73:0124009
31. De K, Thakur M, Manna A, Giri S (2006) J Appl Phys 99:013908